



**The Structure and Activation of Substrate Water Molecules  
in Sr<sup>2+</sup>-Substituted Photosystem II.**

Journal:	<i>Physical Chemistry Chemical Physics</i>
Manuscript ID:	CP-ART-07-2014-003082.R1
Article Type:	Paper
Date Submitted by the Author:	07-Aug-2014
Complete List of Authors:	Lakshmi, K. V.; Rensselaer Polytechnic Institute, Chemistry and Chemical Biology Chatterjee, Ruchira; Rensselaer Polytechnic Institute, Chemistry and Chemical Biology Milikisiyants, Sergey; Rensselaer Polytechnic Institute, Chemistry and Chemical Biology Coates, Christopher; Rensselaer Polytechnic Institute, Chemistry and Chemical Biology Shen, J.-R.; Okayama University, Department of Biology Koua, Faisal; Okayama University, Division of Bioscience

The Structure and Activation of Substrate Water Molecules in Sr<sup>2+</sup>-Substituted  
Photosystem II.<sup>†</sup>

Ruchira Chatterjee,<sup>1,3</sup> Sergey Milikisiyants,<sup>1</sup> Christopher S. Coates,<sup>1</sup> Faisal H. M. Koua,<sup>2</sup> Jian-  
Ren Shen<sup>2</sup> & K. V. Lakshmi<sup>1,\*</sup>

<sup>1</sup>Department of Chemistry and Chemical Biology and

The Baruch '60 Center for Biochemical Solar Energy Research

Rensselaer Polytechnic Institute

Troy, NY 12180

<sup>2</sup>Photosynthesis Research Center

Graduate School of Natural Science and Technology and Faculty of Science

Okayama University

Okayama 700-8530, Japan

<sup>3</sup>Present Address: Physical Biosciences Division □

Lawrence Berkeley National Laboratory

Berkeley, CA 94720

TITLE RUNNING HEAD: Two-Dimensional <sup>1</sup>H HYSCORE Spectroscopy of the S<sub>2</sub> State of  
Photosystem II.

†This study is supported by the Photosynthetic Systems Program, Office of Basic Energy Sciences, United States Department of Energy (DE-FG02-07ER15903) (K.V.L.) and by a Grant-in-Aid for Specially Promoted Research No. 24000018 from MEXT/JSPS of Japan (J.R.S.).

\* Author for Correspondence:

K. V. Lakshmi

Department of Chemistry and Chemical Biology

Rensselaer Polytechnic Institute

Troy, NY 12180

Phone: (518) 276 3271

Fax: (518) 276 4887

Email: [lakshk@rpi.edu](mailto:lakshk@rpi.edu)

Key Words: Photosystem II, solar water oxidation, S<sub>2</sub> state, tetra-nuclear manganese calcium-oxo (Mn<sub>4</sub>Ca-oxo) cluster, EPR spectroscopy, ESEEM spectroscopy, HYSCORE spectroscopy.

**ABSTRACT.**

The mechanism of solar water oxidation by photosystem II (PSII) is of fundamental interest and it is the object of extensive studies both in the past and present. The solar water oxidation reaction of PSII occurs in the oxygen-evolving complex (OEC). The OEC consists of a tetranuclear manganese calcium-oxo ( $\text{Mn}_4\text{Ca-oxo}$ ) cluster that is surrounded by amino acid residues and inorganic cofactors. The role of the  $\text{Ca}^{2+}$  ion in the water oxidation reaction is one of the most interesting questions that is yet to be answered. In this study, we probe the structural and functional differences induced by metal ion substitution in the  $\text{Mn}_4\text{Ca-oxo}$  cluster by substituting the  $\text{Ca}^{2+}$  ion in the OEC by a  $\text{Sr}^{2+}$  ion. We apply two-dimensional (2D) hyperfine sublevel correlation (HYSCORE) spectroscopy to detect weak magnetic interactions between the paramagnetic  $\text{Mn}_4\text{Sr-oxo}$  cluster and the surrounding protons in the  $S_2$  state of the OEC of  $\text{Sr}^{2+}$ -substituted PSII. We identify three groups of protons that are magnetically interacting with the  $\text{Mn}_4\text{Sr-oxo}$  cluster. Using the recently reported 1.9 Å resolution X-ray structure of the OEC in the  $S_1$  state [Umena et al., *Proc. Natl. Acad. Sci. U.S.A.*, 2013, **110**, 3889] and the high-resolution 2D HYSCORE spectroscopy studies of the  $S_2$  state of the OEC of  $\text{Ca}^{2+}$ -containing PSII [Milikisiyants et al., *Energy Environ. Sci.*, 2012, **5**, 7747], we discuss the assignments of the three groups of protons that are magnetically coupled to the  $\text{Mn}_4\text{Sr-oxo}$  cluster. Since hyperfine interactions are highly sensitive to small perturbations in the electronic and geometric structure of paramagnetic centers, a comparison of the 2D HYSCORE spectra of  $\text{Sr}^{2+}$ -substituted and  $\text{Ca}^{2+}$ -containing PSII allows us to draw important conclusions with respect to the structure of the substrate water molecules in the OEC and the role of the  $\text{Ca}^{2+}$  ion in the water oxidation reaction. In addition, for the first time, we determine the experimental value of the spin projection factor

for the Mn(III) ion of the Mn<sub>4</sub>Ca-oxo cluster as  $\rho_1 = \pm 1.7$  from the assignment of the hyperfine interaction of the paramagnetic cluster with the protons of the D1-His332 residue of PSII.

## INTRODUCTION.

The photosynthetic water oxidation reaction is catalyzed by the oxygen-evolving complex (OEC) that is located on the luminal side of photosystem II (PSII).<sup>1-5</sup> In comparison with existing artificial water splitting catalysts, the OEC has unrivaled efficiency and turnover rates that require only moderate activation energies. The OEC consists of a tetranuclear manganese calcium-oxo ( $\text{Mn}_4\text{Ca-oxo}$ ) cluster that is surrounded by a protein environment. During the solar water oxidation reaction, the OEC cycles through five different oxidation states  $S_0 - S_4$ .<sup>6</sup> The X-ray crystal structure of the dark stable  $S_1$  state was recently resolved at 1.9 Å resolution.<sup>7</sup> The high-resolution X-ray crystal structure has allowed for the determination of the geometry of the  $\text{Mn}_4\text{Ca-oxo}$  cluster and the amino acid and water ligands that are coordinated to the catalytic cluster. In the  $\text{Mn}_4\text{Ca-oxo}$  cluster, three manganese ions and the  $\text{Ca}^{2+}$  ion form a distorted cubane while the fourth manganese ion is “dangler”. Despite the remarkable breakthrough of the high-resolution structure of PSII in the  $S_1$  dark state, the detailed mechanism of the solar water oxidation reaction remains unknown.

The role of the  $\text{Ca}^{2+}$  ion in the water oxidation reaction is one of the most interesting questions that is yet to be answered. It is well known that the  $\text{Ca}^{2+}$  ion is crucial for the water oxidation reaction in the OEC of PSII. After removal of the  $\text{Ca}^{2+}$  ion,  $S_2$  state of the OEC is observed, however, the formation of the higher oxidation S state intermediates is blocked.<sup>8, 9</sup> There are three possible roles that have been suggested for the  $\text{Ca}^{2+}$  ion in the OEC of PSII: (i) the positive charge of the  $\text{Ca}^{2+}$  ion is required to level the reduction potential of the  $\text{Mn}_4\text{Ca-oxo}$  cluster in the OEC,<sup>10-13</sup> (ii) the presence of the  $\text{Ca}^{2+}$  ion is required for maintaining the structure of the  $\text{Mn}_4\text{Ca-oxo}$  cluster and/or hydrogen-bonding network in the OEC, thus allowing efficient proton

transfer<sup>14, 15</sup> and (iii) a water or hydroxide ion bound to the  $\text{Ca}^{2+}$  ion acts as a nucleophile during the formation of the oxygen-oxygen bond in the water oxidation reaction.<sup>16-18</sup>

The structural and functional differences induced by metal ion substitution could provide valuable insight into the role of the  $\text{Ca}^{2+}$  ion in the water oxidation reaction in the OEC of PSII.<sup>12, 14, 16, 19-24</sup> Upon substitution of the  $\text{Ca}^{2+}$  ion, the only divalent ion that is capable of restoring catalytic activity in the OEC is the  $\text{Sr}^{2+}$  ion.<sup>12, 16, 25-27</sup> However, the catalytic turnover is slower upon  $\text{Ca}^{2+}$  to  $\text{Sr}^{2+}$  ion substitution.<sup>12, 13, 19</sup> It has been proposed that  $\text{Sr}^{2+}$  is a functional replacement of the  $\text{Ca}^{2+}$  ion in the OEC based on (a) similar ionic radius and (b) similar Lewis acidity.<sup>16</sup> The effect of  $\text{Ca}^{2+}$  to  $\text{Sr}^{2+}$  ion substitution has previously been studied by time-resolved membrane-inlet mass spectrometry using  $\text{H}_2^{16}\text{O}/\text{H}_2^{18}\text{O}$  isotope exchange.<sup>15, 28, 29</sup> It was demonstrated that the exchange kinetics of the slowly exchanging substrate water molecule is ~ 3 - 4 times faster in  $\text{Sr}^{2+}$ -substituted PSII suggesting that one of the two substrate water molecules is bound to the  $\text{Ca}^{2+}$  ion in the OEC. The spectroscopic properties of  $\text{Sr}^{2+}$ -substituted PSII have been studied by electron paramagnetic resonance (EPR) and EXAFS spectroscopy.<sup>12, 14, 20, 24, 30</sup> Initially, the differences in the electron-nuclear hyperfine pattern that was observed in the multiline EPR signal in the  $\text{S}_2$  state of the OEC were attributed to significant changes in the electronic structure that are induced by  $\text{Sr}^{2+}/\text{Ca}^{2+}$  ion substitution.<sup>12</sup> However, comparison of the EXAFS spectra of  $\text{Sr}^{2+}$ -substituted and  $\text{Ca}^{2+}$ -containing PSII has revealed little difference in the molecular structure of the OEC.<sup>20</sup> This study suggested only small elongation of the Mn-Sr distance of ~ 0.1 Å. In a recent study, the electronic structure of the  $\text{Mn}_4\text{Sr}$ -oxo cluster in the  $\text{S}_2$  state was studied using a combination of conventional field-sweep EPR spectroscopy, pulsed  $^{55}\text{Mn}$  electron nuclear double resonance (ENDOR) spectroscopy and advanced density functional theory (DFT) calculations.<sup>24</sup> It was found that the electronic structure of the catalytic cluster

remains unaffected by the replacement of the  $\text{Ca}^{2+}$  ion by  $\text{Sr}^{2+}$  and that subtle changes in the hyperfine anisotropy of the Mn(III) ion (referred to as the Mn1 ion in the high-resolution X-ray crystal structure of PSII)<sup>7</sup> are responsible for small differences that are observed in the multiline EPR signal of the  $\text{S}_2$  state of the OEC. Recently, the X-ray crystal structure of the dark stable  $\text{S}_1$  state of  $\text{Sr}^{2+}$ -substituted PSII has been resolved at 2.1 Å resolution and compared with the X-ray crystal structure of native  $\text{Ca}^{2+}$ -containing PSII.<sup>31</sup> In agreement with earlier EXAFS findings, the molecular structure of the  $\text{Mn}_4\text{Ca}$ -oxo cluster was found to be nearly unperturbed by metal ion substitution. Although the crystallographic data indicate that the structure of native  $\text{Ca}^{2+}$ -containing and  $\text{Sr}^{2+}$ -substituted PSII is similar, there are structural differences that are clearly resolved within the OEC. It has been found that the position of  $\text{Sr}^{2+}$  ion is shifted towards the outside of the distorted cubane by  $\sim 0.3$  Å in comparison with the position of the  $\text{Ca}^{2+}$  ion in native PSII. In addition, one of the water molecules that is directly coordinated to the  $\text{Ca}^{2+}$  ion is shifted by 0.2 - 0.3 Å from the metal ion upon  $\text{Sr}^{2+}$  substitution that suggests weaker binding and higher mobility of the water molecule.

While EPR and EXAFS spectroscopy as well as the recent high-resolution X-ray crystal structures of PSII clearly demonstrate that the molecular and electronic structure of the  $\text{Mn}_4\text{Ca}$ -oxo cluster remains essentially unchanged upon  $\text{Sr}^{2+}$  ion substitution, transient optical absorption spectroscopy in combination with electron spin echo envelope modulation (ESEEM) spectroscopy suggests that the hydrogen-bonding network connecting the  $\text{Mn}_4\text{Sr}$ -oxo cluster and redox-active tyrosine residue,  $\text{Y}_Z$ , is perturbed upon substitution of the  $\text{Ca}^{2+}$  ion by  $\text{Sr}^{2+}$  which hinders the water oxidation reaction.<sup>14</sup>

In this study, we apply two-dimensional (2D) hyperfine sub-level correlation (HYSCORE) spectroscopy to probe the structural changes in the  $\text{S}_2$  state of the OEC of  $\text{Sr}^{2+}$ -substituted PSII.

In comparison with one-dimensional EPR techniques, 2D HYSCORE spectroscopy provides enhanced resolution with respect to simultaneous detection of multiple magnetic nuclei interacting with the paramagnetic catalytic cluster in the OEC. This is possible as the overlapping signals are better separated due to the presence of an extra dimension. In our previous investigations, we have successfully used 2D HYSCORE spectroscopy to detect hyperfine interactions of the Mn<sub>4</sub>Ca-oxo cluster with the surrounding <sup>14</sup>N and <sup>1</sup>H nuclei in native Ca<sup>2+</sup>-containing PSII.<sup>32,33</sup> We had determined the weak magnetic fields induced by three distinct <sup>14</sup>N atoms and five groups of protons in the photochemically trapped S<sub>2</sub> state of the OEC. Interestingly, two of the groups of protons display a significant isotropic hyperfine interaction and were assigned to the two water ligands that are coordinated to the Mn<sub>4</sub>Ca-oxo cluster in the S<sub>2</sub> state of the OEC. In addition, one of the groups of protons was found to be in close proximity of the Mn<sub>4</sub>Ca-oxo cluster and was assigned to either a water ligand of the Ca<sup>2+</sup> ion or to two nearest protons of the D1-His332 residue in the OEC. Since hyperfine interactions are highly sensitive to small perturbations in the electronic and geometric structure of paramagnetic centers, a comparison of the 2D HYSCORE spectra of Sr<sup>2+</sup>-substituted and Ca<sup>2+</sup>-containing PSII allows us to draw important conclusions with respect to the structure of the substrate water molecules in the OEC and the role of the Ca<sup>2+</sup> ion in the water oxidation reaction.

## **MATERIALS AND METHODS.**

### ***Preparation of Sr<sup>2+</sup>-substituted Photosystem II.***

Sr<sup>2+</sup>-substituted PSII from *Thermosynechococcus vulcanus* was prepared as follows. The *T. vulcanus* cells were grown at 47.0 ± 2.0 °C in 40 L of medium containing 0.8 mM Sr<sup>2+</sup> ions in the absence of Ca<sup>2+</sup> ions for one week.<sup>19,34</sup> The thylakoid membranes and PSII core complexes

were prepared according to previously published procedures<sup>34,35</sup> with buffers containing  $\text{Sr}^{2+}$  in place of  $\text{Ca}^{2+}$  ions (except for the buffers used for column chromatography where  $\text{Ca}^{2+}$ -containing buffers were used, please see ref. 17 and 32). The purified  $\text{Sr}^{2+}$ -substituted PSII was washed with buffer containing  $\text{Sr}^{2+}$  instead of  $\text{Ca}^{2+}$  ions (5.0 % glycerol, 20.0 mM MES-NaOH pH 6.1, 20.0 mM NaCl, 3.0 mM  $\text{SrCl}_2$ ) and finally suspended in the same buffer to concentrations of 6.0-10.0 mg Chl/ml. The  $\text{Sr}^{2+}$ -substituted PSII was stored in liquid  $\text{N}_2$  in the dark prior to the pulsed EPR spectroscopy measurements.

### ***Trapping of the Photochemical $S_2$ State of $\text{Sr}^{2+}$ -substituted Photosystem II.***

The  $\text{Sr}^{2+}$ -substituted PSII complexes from *Thermosynechococcus vulcanus* were resuspended in buffer containing 5.0 % glycerol, 20.0 mM MES-NaOH pH 6.1, 20.0 mM NaCl and 3.0 mM  $\text{SrCl}_2$ . The PSII samples were pre-incubated with 200  $\mu\text{M}$  potassium ferricyanide prior to illumination. The  $S_2$  state was cryo-trapped by illumination for 2 minutes at 200 K followed by rapid freezing (5 -10 s) at 77 K in the dark.<sup>32, 33, 36-40</sup> The  $S_1$  state was accumulated by dark-adapting PSII at 0° C for 30 minutes.

### ***Pulsed EPR Spectroscopy.***

The EPR spectra were recorded on a custom-built continuous-wave (cw)/pulsed X-band Bruker Elexsys 580 spectrometer. The details of the spectrometer are described in previous literature.<sup>32, 33, 41-44</sup> All of the pulsed EPR spectra were acquired at 5 K.

For the electron spin-echo-detected magnetic field-sweep EPR spectra, the primary electron spin echo was generated using the pulse sequence ( $\pi/2$ - $\tau$ - $\pi$ -echo). The echo was integrated over a 40 ns time window that was centered at the maximum of the echo signal. The length of the  $\pi/2$ - and

$\pi$ -pulse was 12 ns and 24 ns, respectively. The inter-pulse separation,  $\tau$ , was 144 ns and the delay in the pulse sequence is defined as the difference in the starting point of the pulses.

For the HYSCORE spectra, the echo amplitude was measured using the pulse sequence ( $\pi/2$ - $\tau$ - $\pi/2$ - $t_1$ - $\pi$ - $t_2$ - $\pi/2$ -echo) with an 8 ns and 16 ns length for the  $\pi/2$ - and  $\pi$ -pulse, respectively, and an 8 ns detector gate (that is centered at the maximum of the echo signal). The delays in the pulse sequence are defined as the difference in the starting point of the pulses. The echo intensity was measured as a function of  $t_1$  and  $t_2$ , where  $t_1$  and  $t_2$  were incremented in steps of 16 ns from an initial value of 40 ns and 32 ns, respectively. 256 steps were used for each dimension. The 8 ns time difference between the initial value of  $t_1$  and  $t_2$  was set to account for the difference in length between the  $\pi/2$ - and  $\pi$ -pulse. This provided symmetric spectra in both dimensions. The unwanted echoes and anti-echoes were eliminated by applying a 16-step phase cycling procedure. A third order polynomial baseline was subtracted from the resulting time-domain spectra. The corrected spectra were zero-filled to obtain [2048 x 2048] matrix and Fourier transformed using a Fast Fourier Transformation (FFT) algorithm. The frequency domain spectra were plotted as the amplitude (absolute value).

The 2D  $^1\text{H}$  HYSCORE spectra were recorded at magnetic field of 337.5 mT (effective g value of 1.95) with an inter-pulse delay,  $\tau$ , of 140 ns (this is the delay between the first and second pulse). The choice of the inter-pulse delay was mandatory since useful spectral information can only be obtained when the contribution due to matrix nuclei is suppressed by matching the blind-spot frequency to the proton Zeeman frequency ( $\nu_Z = 14.37$  MHz). To match the blind-spot frequency and the proton Zeeman frequency, the inter-pulse delay,  $\tau$ , must satisfy the condition  $\tau = N/\nu_Z$  (where  $N = 1, 2, 3, \dots$ ), thus  $\tau$  has to be  $N \cdot 70$  ns. Since  $\tau$  value of 70 ns is too short to avoid the

ring down of the resonator, the shortest  $\tau$  that yields practical results is 140 ns. If the condition,  $\tau = N/v_z$ , is not matched then there is an intense signal from matrix protons that dominates the 2D  $^1\text{H}$  HYSCORE spectrum which masks important spectral information.

The 2D  $^1\text{H}$  HYSCORE spectra were analyzed as described in a previous study of the  $S_2$  state of OEC of  $\text{Ca}^{2+}$ -containing PSII.<sup>33</sup> Briefly, the 2D  $^1\text{H}$  HYSCORE spectra were plotted in frequency-squared coordinates where the proton ridges become segments of straight lines. From the slope and the intercept of the straight line, we obtained the possible sets of the isotropic ( $a_{\text{iso}}$ ) and anisotropic (T) component of electron-nuclear hyperfine tensor. The right set of hyperfine parameters were selected based on previous studies of the  $S_2$  state of the OEC of PSII and mixed-valence dimanganese di- $\mu$ -oxo models by pulsed EPR spectroscopy.<sup>33, 42</sup>

## RESULTS.

### *Electron Spin-Echo-Detected Magnetic Field-Sweep EPR Spectra of $\text{Sr}^{2+}$ -substituted Photosystem II.*

At room temperature, the OEC of PSII cycles through five light-driven “charge-storage” or S states that results in the oxidation of two molecules of water to dioxygen.<sup>6</sup> The transition from the  $S_1$  to the  $S_2$  state involves electron transfer from the  $\text{Mn}_4\text{Ca}$ -oxo cluster to the redox-active tyrosine residue,  $Y_Z$ , in the OEC of PSII. However, the transition from the  $S_2$  to the  $S_3$  state is proposed to involve both proton and electron transfer reactions. The proton transfer reaction is blocked at 200 K, which allows for the cryogenic trapping of the  $S_2$  state of the  $\text{Mn}_4\text{Ca}$ -oxo cluster for spectroscopic measurements.<sup>38-40, 45</sup>

Shown in Figure 1 is the electron spin-echo-detected magnetic field-sweep EPR spectrum that is obtained as a difference of the  $S_2$  minus  $S_1$  state of  $Sr^{2+}$ -substituted PSII. The spectrum is centered at  $g \sim 2$  with a spectral width of  $\sim 180$  mT. The spectral line shape is similar to the EPR spectrum that was previously reported for the  $S_2$  state of the  $Mn_4Ca$ -oxo and  $Mn_4Sr$ -oxo cluster in the OEC of  $Ca^{2+}$ -containing and  $Sr^{2+}$ -substituted PSII, respectively.<sup>14, 19, 32, 33, 46</sup> The multiline pattern that is observed in the field-sweep EPR spectrum (Figure 1) is characteristic of the  $S_2$  state of the OEC and arises from the electron nuclear hyperfine interactions of the paramagnetic  $Mn_4Sr$ -oxo cluster (electron spin  $S = 1/2$ ) with the four paramagnetic  $^{55}Mn$  ions (nuclear spin  $I = 5/2$ ).<sup>38-40, 45</sup> The multiline EPR signal from the  $S_2$  state is accompanied by a narrow intense signal that is centered at  $g \sim 2.005$ . This signal arises from the dark-stable tyrosyl radical ( $Y_D^\bullet$ ) of PSII.<sup>32</sup> In addition, there is a possible contribution of the primary semiquinone,  $Q_A^-$ , that is magnetically coupled to the high-spin non-heme Fe(II) center of PSII in the spectral region corresponding to  $g \leq 2$ .<sup>32</sup> There is also a small microwave cavity artifact that appears at the high-field edge of the multiline field-sweep EPR spectrum (effective  $g \sim 1.7$ ). As can be seen in Figure 1, there is no contribution from the oxidized heme center of Cyt  $b_{559}$  in the difference spectrum as Cyt  $b_{559}$  was completely pre-oxidized in the  $S_1$  state. The spectral contributions from the  $Y_D^\bullet$  and  $Q_A^-$  semiquinone cofactor to the 2D  $^1H$  HYSCORE spectra are avoided by acquisition of the 2D HYSCORE spectra at a magnetic field position that corresponds to an effective  $g$  value of 2.05 (marked by an arrow in Figure 1). Importantly, the multiline field-sweep EPR signal from  $S_2$  state of the OEC has nearly the highest intensity at this spectral position.

### ***2D $^{14}N$ and $^1H$ HYSCORE Spectroscopy of the $S_2$ State of $Sr^{2+}$ -substituted Photosystem II.***

The complete 2D HYSCORE spectra of dark-adapted and illuminated  $\text{Sr}^{2+}$ -substituted PSII that are acquired at 337.5 mT ( $g = 2.05$ ) are shown in the Figure 1SA and Figure 1SB, respectively, in the Supporting Information. The spectra are similar to the 2D HYSCORE spectra of dark-adapted and illuminated  $\text{Ca}^{2+}$ -containing PSII that was recently reported in literature.<sup>32</sup> All of the spectral features in Figure 1SB that arise upon cryogenic illumination of  $\text{Sr}^{2+}$ -substituted PSII are due to electron-nuclear hyperfine couplings of the paramagnetic  $\text{Mn}_4\text{Sr}$ -oxo cluster in the  $S_2$  state (electron spin  $S = 1/2$ ) of the OEC with the nuclear spins of the surrounding  $^{14}\text{N}$  (nuclear spin  $I = 1$ ) and  $^1\text{H}$  ( $I = 1/2$ ) atoms.

In the  $(-,+)$  quadrant of the spectrum shown in Figure 1SB, there is a pronounced pair of ridges that arises from double quantum (DQ) transitions of an  $^{14}\text{N}$  nucleus that is magnetically interacting with the  $\text{Mn}_4\text{Sr}$ -oxo cluster in the  $S_2$  state of the OEC. The ridges are marked with arrows in Figure 1SB. The ridges in Figure 1SB are assigned entirely to the  $S_2$  state of the  $\text{Mn}_4\text{Sr}$ -oxo cluster as there is no appreciable overlapping intensity that is observed from the dark stable  $S_1$  state in Figure 1SA. Figure 2 shows a comparison of the position of the DQ ridges that are obtained for  $\text{Ca}^{2+}$ -containing PSII and  $\text{Sr}^{2+}$ -substituted PSII under identical experimental conditions. The position of DQ ridges of  $\text{Sr}^{2+}$ -substituted PSII are nearly identical to the ridges that are observed for the strongly interacting  $^{14}\text{N}$  nucleus in the  $S_2$  state of the OEC of  $\text{Ca}^{2+}$ -containing PSII.<sup>32</sup> There is a small shift of  $\sim 0.1$  MHz towards higher frequency that is detected upon comparison of the spectra in Figure 2. In a previous  $^{14}\text{N}$  HYSCORE investigation, we obtained the range of possible electron-nuclear hyperfine and quadrupole parameters for the strongly interacting  $^{14}\text{N}$  nucleus in the  $S_2$  state of OEC of  $\text{Ca}^{2+}$ -containing PSII.<sup>32</sup> The difference in the position of DQ ridges for  $\text{Sr}^{2+}$ -substituted PSII in comparison with  $\text{Ca}^{2+}$ -containing PSII ( $\sim 0.1$  MHz) is much smaller than the range of uncertainty of the hyperfine parameters determined

here and is within sample-to-sample variation. The position of the DQ ridges is very sensitive to any change in the hyperfine interaction between the paramagnetic center and the  $^{14}\text{N}$  nucleus.<sup>47</sup> Thus, we conclude that the difference in the hyperfine interaction of the strongly interacting nitrogen atom is negligible for  $\text{Sr}^{2+}$ -substituted and  $\text{Ca}^{2+}$ -containing PSII.

Shown in Figure 3 is the 2D  $^1\text{H}$  HYSCORE spectrum of the  $S_2$  state of the OEC of  $\text{Sr}^{2+}$ -substituted PSII. In  $\text{Sr}^{2+}$ -substituted PSII, similar to previous observations with the  $S_2$  state of the OEC of  $\text{Ca}^{2+}$ -containing PSII (Figure 4),<sup>33</sup> the cross-peaks that arise from the electron-nuclear hyperfine interactions of the  $\text{Mn}_4\text{Sr}$ -oxo cluster in the  $S_2$  state with the protons are located only in the (+,+) quadrant in the frequency range centered at the proton Zeeman frequency ( $\nu_p = 14.37$  MHz). This is apparent from a comparison of the skyline projections of the 2D HYSCORE spectra that are observed for the dark stable  $S_1$  state and the illuminated  $S_2$  state as shown in the Figure 2S in the Supporting Information. The proton cross-peaks are located in the 10 - 20 MHz frequency range where there is no appreciable signal intensity that is observed for the dark stable  $S_1$  state.

As can be seen in Figure 3, there are three well-resolved pairs of extended ridges ( $\text{H}^{\text{I}} - \text{H}^{\text{III}}$ ) along with  $\text{H}^{\text{IV}}$  group of protons (not shown in the figure). Each pair of ridges corresponds to a specific group of protons and consists of two ridges that are symmetrically displaced from the main diagonal and are centered at the proton Zeeman frequency of  $\nu_p = 14.37$  MHz. The ridges arising from the  $\text{H}^{\text{I}}$  group of protons display the most pronounced intensity, the longest frequency span and the largest shift from the anti-diagonal that is determined by equation  $\nu_1 + \nu_2 = 2\nu_p$ . The large frequency span and the long shift from the anti-diagonal suggest high anisotropy of the hyperfine interaction. This indicates that the  $\text{H}^{\text{I}}$  group of protons is in close proximity of the paramagnetic core of the  $\text{Mn}_4\text{Ca}$ -oxo cluster. The shift from the anti-diagonal and the frequency

span of the proton ridges due to the H<sup>II</sup> group of protons is of an intermediate size. The length of the ridges is roughly two times smaller than the ridges arising from the H<sup>I</sup> group of protons that indicates that the hyperfine anisotropy of the ridges from H<sup>II</sup> is roughly two times smaller than that of H<sup>I</sup>. The ridges from the H<sup>III</sup> group of protons have the smallest span and are located closest to the anti-diagonal as well as the main diagonal in the spectrum. The ridges from the H<sup>III</sup> group of protons reflect small hyperfine anisotropy and suggest a remote nature of the interacting protons with respect to the Mn<sub>4</sub>Sr-oxo cluster.

In order to determine the hyperfine parameters from the location of the proton ridges in the frequency space, we use linear analysis of the 2D <sup>1</sup>H HYSCORE spectrum of the S<sub>2</sub> state of the OEC of Sr<sup>2+</sup>-substituted PSII that is plotted in frequency-squared coordinates (Figure 3S in the Supporting Information) as described in the experimental section. The details of the linear analysis are described in a previous 2D <sup>1</sup>H HYSCORE spectroscopy study of the S<sub>2</sub> state of the Mn<sub>4</sub>Ca-oxo cluster in Ca<sup>2+</sup>-containing PSII.<sup>33</sup> The values of the isotropic (A<sub>iso</sub>) and anisotropic (T) component of the electron-nuclear hyperfine tensors for the H<sup>I</sup>-H<sup>III</sup> group of protons that are obtained using the linear analyses are presented in Table 1.

## DISCUSSION.

### *Assignment of the 2D <sup>14</sup>N HYSCORE Spectrum of Sr<sup>2+</sup>-substituted Photosystem II.*

In order to assign the 2D <sup>14</sup>N HYSCORE, we consider the hyperfine parameters obtained here in conjunction with previously published pulsed EPR spectroscopy studies of Ca<sup>2+</sup>-containing PSII<sup>32</sup> and the recent 1.9 Å resolution X-ray crystal structure of PSII.<sup>7</sup> The appearance of the <sup>14</sup>N cross-peaks in the (-, +) quadrant of the 2D <sup>14</sup>N HYSCORE spectrum shown in Figure 1SB and

Figure 2A indicates a much stronger electron-nuclear hyperfine interaction of the  $^{14}\text{N}$  nucleus in comparison with the nuclear Zeeman interaction. In the case of  $\text{Ca}^{2+}$ -containing PSII, the  $^{14}\text{N}$  nucleus that is strongly interacting with the paramagnetic core of  $\text{Mn}_4\text{Ca}$ -oxo cluster has been identified as the imino nitrogen of the D1-His332 residue.<sup>32, 48, 49</sup> Similar hyperfine parameters have also previously been observed in multi-frequency ESEEM spectroscopy studies of  $\text{Ca}^{2+}$ -containing PSII.<sup>48</sup> The recent X-ray crystal structure of the dark stable  $\text{S}_1$  state of the OEC, for the first time, provides high-resolution information on the coordination environment of the metal ions in the  $\text{Mn}_4\text{Ca}$ -oxo cluster of PSII. The only nitrogen atom that is directly coordinated at the  $\text{Mn}_4\text{Ca}$ -oxo cluster is from the D1-His332 residue. This is also in agreement with the previously published pulsed EPR spectroscopy studies of the D1-H332E genetic variant of PSII.<sup>50, 51</sup>

The spectral features that are observed for the strongly interacting nitrogen atom in the  $\text{S}_2$  state of the OEC of  $\text{Sr}^{2+}$ -substituted PSII in Figure 2A are very similar to the features that are observed in  $\text{Ca}^{2+}$ -containing PSII (Figure 2B). There is a small difference in the position of the cross-peaks ( $\sim 0.1$  MHz) that is within the experimental error. Thus, we conclude that the  $^{14}\text{N}$  nucleus that is strongly interacting with the  $\text{Mn}_4\text{Sr}$ -oxo cluster in the  $\text{S}_2$  state of the OEC of  $\text{Sr}^{2+}$ -substituted PSII is the imino nitrogen atom of the D1-His332 residue. This is in agreement with the recent structural study which showed that the coordination of D1-His332 to the  $\text{Mn}_4\text{Ca}$ -oxo cluster was not significantly affected by substitution of the  $\text{Ca}^{2+}$  ion with  $\text{Sr}^{2+}$ .<sup>29</sup>

#### *Assignment of the 2D $^1\text{H}$ HYSCORE Spectrum of $\text{Sr}^{2+}$ -substituted Photosystem II.*

In a previous 2D  $^1\text{H}$  HYSCORE spectroscopy study of the  $\text{S}_2$  state of the OEC of  $\text{Ca}^{2+}$ -containing PSII, we observed electron-nuclear hyperfine interactions with five groups of protons for the  $\text{Mn}_4\text{Ca}$ -oxo cluster (Figure 4).<sup>33</sup> Three of the five groups of protons displayed nearly

identical hyperfine parameters with those of the H<sup>I</sup> - H<sup>III</sup> groups of protons that are observed for the S<sub>2</sub> state of the OEC of Sr<sup>2+</sup>-substituted PSII (Figure 3). Thus, we conclude that the hyperfine interactions with three groups of protons have identical assignments in Sr<sup>2+</sup>-substituted and Ca<sup>2+</sup>-containing PSII.

Based on the hyperfine parameters, we had previously assigned the H<sup>I</sup> group of protons to either the ring protons of the proximal D1-His332 residue or protons of the water ligands that are coordinated at the Ca<sup>2+</sup> ion of the Mn<sub>4</sub>Ca-oxo cluster in the S<sub>2</sub> state of the OEC of Ca<sup>2+</sup>-containing PSII.<sup>33</sup> In the latter case, we would expect a significant change in the values of the hyperfine interaction for these protons upon substitution of the Ca<sup>2+</sup> ion with Sr<sup>2+</sup> in the OEC. This is because the position of the Sr<sup>2+</sup> ion with respect to the manganese ions is slightly different in comparison with the Ca<sup>2+</sup> ion and more importantly, Sr<sup>2+</sup> ion substitution affects the coordination geometry of the water ligands.<sup>29</sup> However, the hyperfine parameters do not change upon Sr<sup>2+</sup> ion substitution. This provides strong support that the H<sup>I</sup> group of protons belongs to the two ring protons of the proximal D1-His332 residue. This assignment is in excellent agreement with recent observations on mixed-valence dimanganese Mn(III)Mn(IV) 'di-μ-oxo' complexes.<sup>41</sup> In the present study, the 2D <sup>1</sup>H HYSCORE spectra display nearly identical spectral features from the H<sup>I</sup> group of protons with those that were previously observed from the hyperfine interaction of the protons of the terpyridine ligand that is proximal to the Mn(III) ion in the Mn(III)Mn(IV) 'di-μ-oxo' terpyridine complex.<sup>42</sup>

For the H<sup>II</sup> group of protons that are interacting with the Mn<sub>4</sub>Sr-oxo cluster in the S<sub>2</sub> state of the OEC of Sr<sup>2+</sup>-substituted PSII, based on 2D <sup>1</sup>H HYSCORE spectroscopy of the S<sub>2</sub> state of Ca<sup>2+</sup>-containing PSII we conclude that multiple assignments are possible for the observed hyperfine parameters. Namely, *i*) the protons of a non-coordinated water molecule at a distance of ~ 4 Å or

ii) the protons of the amino acid residues D1-His337 or CP43-Arg357 that are in proximity of the  $\text{Mn}_4\text{Sr}$ -oxo cluster. This assignment is supported by the observation that the hyperfine parameters of the  $\text{H}^{\text{II}}$  group of protons do not display significant changes upon substitution of the  $\text{Ca}^{2+}$  ion with  $\text{Sr}^{2+}$  in the OEC.

Similarly, we assign the  $\text{H}^{\text{III}}$  group of protons to multiple hyperfine interactions of the  $\text{Mn}_4\text{Sr}$ -oxo cluster in the  $\text{S}_2$  state of the OEC with remote matrix protons. This assignment is similar to previous observations in the  $\text{S}_2$  state of the OEC of  $\text{Ca}^{2+}$ -containing PSII.<sup>33</sup> Once again, the hyperfine parameters of the  $\text{H}^{\text{III}}$  group of protons do not significantly change upon substitution of the  $\text{Ca}^{2+}$  ion with  $\text{Sr}^{2+}$  in the OEC. The small values of the hyperfine parameters reflect the remote nature of the  $\text{H}^{\text{III}}$  group of protons and do not provide significant information with respect to the structure of the  $\text{S}_2$  state of the OEC.

Most importantly, in addition to the three groups of proton hyperfine interactions in the  $\text{S}_2$  state of  $\text{Sr}^{2+}$ -substituted PSII, there were two additional important group of protons,  $\text{H}^{\text{IV}}$  and  $\text{H}^{\text{V}}$ , that were detected in the  $\text{S}_2$  state of the OEC of  $\text{Ca}^{2+}$ -containing PSII<sup>33</sup> that are absent in the  $\text{S}_2$  state of the OEC of  $\text{Sr}^{2+}$ -substituted PSII (Figure 3). (Please note that these groups of protons were designated as  $\text{H}^{\text{I}}$  and  $\text{H}^{\text{III}}$  in the previous 2D  $^1\text{H}$  HYSCORE spectroscopy study of  $\text{Ca}^{2+}$ -containing PSII (Figure 4).<sup>33</sup>) Based on the significant value of the isotropic component of the hyperfine interactions of the  $\text{H}^{\text{IV}}$  and  $\text{H}^{\text{V}}$  group of protons, these were assigned to the water ligands that are directly coordinated to one of the manganese ions in the  $\text{Mn}_4\text{Ca}$ -oxo cluster of  $\text{Ca}^{2+}$ -containing PSII.<sup>33</sup> Alternately, the proton(s) could be bound to any of the five oxygen atoms in the  $\mu$ -oxo bridges that connect the four manganese and one calcium ion in the  $\text{Mn}_4\text{Ca}$ -oxo cluster in the OEC. In this case, the respective hyperfine interactions would be highly rhombic in contrast to the nearly axial couplings that are observed for each of the groups of

protons in the present study. Thus, we do not favor protonation of the  $\mu$ -oxo bridges in the  $S_2$  state of the OEC.

The main spectroscopic difference between the  $H^{IV}$  and  $H^V$  groups of protons is the magnitude of the respective hyperfine interactions. The previously measured value of the anisotropic hyperfine component,  $T$ , for the  $H^{IV}$  and  $H^V$  groups of protons in the  $S_2$  state of the OEC of  $Ca^{2+}$ -containing PSII was  $\pm 4.4$  MHz and  $\pm 1.9$  MHz, respectively.<sup>33</sup> In contrast, the isotropic hyperfine component,  $A_{iso}$ , is larger for  $H^V$  ( $A_{iso} = \pm 2.6$  MHz) as compared to a value of  $\pm 1.8$  MHz for the  $H^I$  group of protons. The magnitude of the anisotropic component of the hyperfine interaction for the  $H^{IV}$  group of protons is in agreement with the assignment as a terminal water ligand(s) that is coordinated to the “dangler” manganese ion (denoted as Mn4 in the recent 1.9 Å X-ray crystal structure). A simple point-dipole approximation yields  $\sim 4$  MHz for the absolute magnitude of the anisotropic component of the hyperfine interaction which is very close to the experimentally measured value of  $T = \pm 4.4$  MHz. Thus, we assign the  $H^{IV}$  group of protons to the water ligand(s) that are coordinated at the Mn4 ion. Interestingly, in a recent study by Navarro et al., the authors report that ammonia displaces a water ligand at the Mn4 ion with a +4 oxidation state. With the help of mass spectrometry, the authors exclude the water ligand as a substrate site.<sup>52</sup> In contrast, a much smaller value of the anisotropic component of the hyperfine interaction for the  $H^V$  group of protons ( $T = \pm 1.9$  MHz) requires significant suppression of the dipolar field of the binding Mn by the other Mn ion(s) in the  $Mn_4Ca$ -oxo cluster. In principle, this is possible if the water molecule that is coordinated at one of the Mn(IV) ions is located in the vicinity and antiferromagnetically coupled to the only Mn(III) ion in the cluster. In mixed-valence Mn(III)-Mn(IV) dimanganese di- $\mu$ -oxo model systems, we have previously observed significant suppression of the anisotropic hyperfine interaction of the terminal water ligand

bound to a Mn(IV) ion due to the presence of an antiferromagnetically coupled Mn(III) ion in the vicinity.<sup>42</sup> Such a possibility would exist only for the ions denoted as Mn2 and Mn3 in the X-ray crystal structure and require significant rearrangement of the cluster upon the  $S_1$  to  $S_2$  state transition of the  $Mn_4Ca$ -oxo of the OEC. This is not supported by previous EXAFS measurements.<sup>20</sup> The assignment of the  $H^V$  group of protons will be further investigated in future studies.

Since the 2D  $^1H$  HYSCORE cross-peaks from the water ligands are absent in the  $S_2$  state of the OEC of  $Sr^{2+}$ -substituted PSII while all of the other cross-peaks remain virtually unchanged, the difference between the two spectra provides us with the pure 2D  $^1H$  HYSCORE spectrum of the water molecules that are coordinated to  $Mn_4Ca$ -oxo cluster of the OEC. The 2D  $^1H$  HYSCORE difference spectrum between the  $S_2$  state of  $Ca^{2+}$ -containing PSII and  $Sr^{2+}$ -substituted PSII is shown in the Figure 4S. The spectrum is plotted in frequency-squared coordinates in Figure 5S. The hyperfine parameters that are determined from the difference spectrum are identical within experimental error to the hyperfine parameters that were previously determined for the  $S_2$  state of  $Ca^{2+}$ -containing PSII.<sup>33</sup>

*The Relationship to the Structure of OEC in the  $S_2$  State and the Role of the  $Ca^{2+}$  Ion in the Solar Water Oxidation Reaction of Photosystem II.*

The hyperfine parameters that are obtained from the 2D HYSCORE spectra of  $Sr^{2+}$ -substituted PSII provide valuable insight into the structure of the OEC in the  $S_2$  state and the possible role of the  $Ca^{2+}$  ion in the catalytic water oxidation reaction of PSII. The structural changes induced by the replacement of the  $Ca^{2+}$  ion in the OEC with  $Sr^{2+}$  is of particular interest, since  $Sr^{2+}$  is the only functional replacement that supports water oxidation in PSII. Importantly, the replacement

of the  $\text{Ca}^{2+}$  ion by  $\text{Sr}^{2+}$  decreases the rate of oxygen evolution of PSII.<sup>12, 13, 19</sup> It has been suggested that the transition from  $S_3$  to  $S_0$  state is slower for  $\text{Sr}^{2+}$ -substituted PSII, however, there is experimental evidence that the earlier steps of the catalytic cycle are also affected by the replacement of the  $\text{Ca}^{2+}$  ion in the OEC of PSII.<sup>12</sup>

Thus far, only subtle structural changes that are induced by  $\text{Sr}^{2+}$  ion replacement have been suggested by X-ray crystallography and EPR spectroscopy. Although  $\text{Sr}^{2+}$  ion replacement in the OEC results in significant modification of the hyperfine pattern of the  $S_2$  state multiline signal that is detected by *cw* EPR spectroscopy, negligible structural perturbations were detected by EXAFS and  $^{55}\text{Mn}$  ENDOR spectroscopy studies.<sup>20, 24</sup> The geometry of the four Mn ions in the  $\text{Mn}_4\text{Ca}(\text{Sr})$ -oxo cluster is proposed to be identical in  $\text{Ca}^{2+}$ -containing and  $\text{Sr}^{2+}$ -substituted PSII. A slight elongation of the Mn-Sr distances on the order of  $\sim 0.1 \text{ \AA}$  have been detected by EXAFS spectroscopy.<sup>20</sup> The modified  $S_2$  multiline EPR spectrum of  $\text{Sr}^{2+}$ -substituted PSII has been attributed to small changes in the anisotropy of the hyperfine interaction with one of four manganese ions in the cluster. Based on a comparison of the  $^{55}\text{Mn}$ -ENDOR spectra, Messinger, Lubitz and coworkers have concluded that besides a subtle reduction of the zero-field splitting (ZFS) interaction in the Mn(III) ion, the electronic structure of the OEC in  $S_2$  state of  $\text{Ca}^{2+}$ -containing and  $\text{Sr}^{2+}$ -substituted PSII are nearly identical.<sup>24</sup>

Most recently, the high-resolution X-ray crystal structures of the OEC in the dark adapted  $S_1$  state has facilitated a detailed comparison between the structure of the OEC of  $\text{Ca}^{2+}$ -containing and  $\text{Sr}^{2+}$ -substituted PSII.<sup>31</sup> Despite the similarity of the X-ray crystal structures, there are three differences that are resolved in these studies. First, the position of the  $\text{Sr}^{2+}$  ion is slightly shifted ( $\sim 0.3 \text{ \AA}$ ) towards the outside of the distorted cubane in comparison with the  $\text{Ca}^{2+}$  ion. This is in agreement with the larger ionic radius of the  $\text{Sr}^{2+}$  ion. Second, one of the water ligands that is

coordinated at the  $\text{Sr}^{2+}$  ion (W3 in the X-ray crystal structure) has an elongated bond length that suggests the involvement of this water molecule in O-O bond formation in the water oxidation reaction.<sup>31</sup> Finally, due to the shift in the position of W3, the hydrogen-bond between W3 and W2, a water ligand bound to Mn4, was broken in the  $\text{Sr}^{2+}$ -substituted PSII.<sup>29</sup>

The results obtained here are in agreement with previous EXAFS and  $^{55}\text{Mn}$  ENDOR studies and the recently resolved X-ray crystal structures of PSII. The hyperfine interaction of the paramagnetic core of the  $\text{Mn}_4\text{Ca}$ -oxo cluster with the  $^{14}\text{N}$  ligand is identical in the  $S_2$  state of  $\text{Ca}^{2+}$ -containing and  $\text{Sr}^{2+}$ -substituted PSII. The hyperfine interaction of the imino nitrogen of the D1-His332 residue is very sensitive to any perturbation of geometry as well as electronic structure of the  $\text{Mn}_4\text{Ca}$ -oxo cluster. Hence, any change of the metal to ligand distance or more importantly, a redistribution of the electron spin density or exchange couplings between the four manganese ions in the  $\text{Mn}_4\text{Ca}(\text{Sr})$ -oxo cluster would result in a change of the observed hyperfine parameters. Thus, based on the comparison of the 2D  $^{14}\text{N}$  HYSCORE spectra of the  $S_2$  state of  $\text{Ca}^{2+}$ -containing and  $\text{Sr}^{2+}$ -substituted PSII, we confirm that the geometry and electronic structure of the  $\text{Mn}_4\text{Ca}(\text{Sr})$ -oxo cluster is not significantly affected upon  $\text{Sr}^{2+}$  ion replacement.

A more detailed comparison is afforded by the 2D  $^1\text{H}$  HYSCORE spectra of  $\text{Sr}^{2+}$ -substituted and  $\text{Ca}^{2+}$ -containing PSII. First, a comparison of the spectra obtained for  $\text{Ca}^{2+}$ -containing and  $\text{Sr}^{2+}$ -substituted PSII allow for the assignment of the most pronounced pair of ridges in the 2D  $^1\text{H}$  HYSCORE spectrum shown in Figure 3, namely, the  $\text{H}^{\text{I}}$  group of protons. The  $\text{H}^{\text{I}}$  group of protons displays a value of nearly zero for the isotropic component of the hyperfine interaction and a value of  $\pm 4.1$  MHz for the anisotropic component, T. This indicates that the  $\text{H}^{\text{I}}$  group of protons are from the proximal D1-His332 residue that is directly coordinated to the  $\text{Mn}_4\text{Ca}(\text{Sr})$ -oxo cluster.

The distance of these protons of the D1-His332 residue coordinated to the manganese ion in the  $\text{Mn}_4\text{Ca}$ -oxo cluster (denoted as Mn1 in the recent 1.9 Å crystal structure depicted in Figure 5) is  $\sim 3.3$  Å. Based on the magnitude of the anisotropic component of the hyperfine interaction, we estimate the spin projection factor of the Mn1 ion in the  $S_2$  state of the OEC. Since we know the distance between the Mn ion and the two protons, and those between the two protons and all of the other Mn ions are  $> 4$  Å, as a first approximation we neglect the contributions from these residues to the hyperfine interaction that is observed in this study. Thus, using a simple point-dipole approximation we obtain the spin projection factor of  $\rho_1 = \pm 1.9$  for the Mn1 ion. Similarly, we can determine the spin projection factor of the “dangler” Mn4 ion. The distances between the protons of the water ligands and the Mn4 ion are  $\sim 2.7$  Å which yields a spin projection factor of  $\rho_4 = \pm 1.1$ . Previous  $^{55}\text{Mn}$  ENDOR spectroscopy studies have reported a range of possible values of  $\rho_1$  of 1.39 - 1.89 and  $\rho_4$  to be one of the three possibilities 0.99 - 1.34, 0.82 - 1.11 and 0.75 - 1.02.<sup>24</sup> The range of values obtained in these studies is relatively broad since it is not possible to directly measure the intrinsic hyperfine interaction for a  $^{55}\text{Mn}$  nucleus. Thus, the value was estimated from the data that is available in literature on monomeric Mn(III) and Mn(IV) model systems. Interestingly in this work, the authors used the structural model proposed by Siegbahn and coworkers.<sup>53</sup> By fitting the 2009 Siegbahn model to the experimental data, the authors calculated the isotropic component of the spin projection tensors as  $\rho_1 = 1.73$  and  $\rho_4 = 1.11$ . This value is in agreement with the present study. In another  $^{55}\text{Mn}$  ENDOR study, Peloquin et al.<sup>54</sup> reported four possible values for the spin projection factor of the Mn(III) ion in the  $S_2$  state as  $\rho_1 = 1.66, 1.77, 0.76, 2.00$ . While the first and the third values do not agree with our estimate of  $\rho_1$ , the second and the last possibilities, namely  $\rho_1 = 1.77$  or 2.00, are in

agreement with the present results. The model proposed by Schinzel et. al has also favored the spin projection factor of the Mn(III) ion to be 1.71.<sup>55</sup>

The values of  $\rho_1$  and  $\rho_4$  that are determined here provide an accurate experimental measurement of the spin projection factors of the Mn1 and Mn4 ions in the OEC in the  $S_2$  state. The knowledge of the spin projection factors is essential for understanding the electronic structure of the  $Mn_4Ca$ -oxo cluster and selection of the proposed theoretical models of water oxidation by PSII. In a recent study, Kulik et al. analyzed available  $^{55}Mn$  ENDOR data in terms of a Y-shaped spin-coupling scheme and arrived upon two possible electronic structures of the  $Mn_4Ca$ -oxo cluster in the  $S_2$  state of the OEC.<sup>56</sup> The main difference between the two structures is the location of the only Mn(III) ion in the  $Mn_4Ca$ -oxo cluster in the  $S_2$  state. In the first model, the Mn(III) ion is the “dangler” Mn ion (Mn4 in the X-ray crystal structure) and in the second model, the Mn(III) ion is coordinating the D1-His332 residue (Mn1 in the X-ray crystal structure). The spin projection factors calculated for these two models are  $\rho_1 = 1.1$  and  $\rho_4 = 1.75$  for the first structure and  $\rho_1 = 1.75$  and  $\rho_4 = 1.1$  for the second structure, respectively. A comparison with our estimates of  $\rho_1$  and  $\rho_4$  allows for discrimination between the two proposed structures rejecting the first possibility as it is not consistent with our experimental observations. Another important difference between the 2D  $^1H$  HYSCORE spectra obtained for the  $S_2$  state of OEC in  $Ca^{2+}$ -containing and  $Sr^{2+}$ -substituted PSII is the disappearance of the cross-peaks that arise from the protons of the water ligands that are directly coordinated at the manganese ion(s). There could be two possible reasons for the differences that we observe in the 2D  $^1H$  HYSCORE spectra of the  $S_2$  state of the OEC of  $Ca^{2+}$ -containing and  $Sr^{2+}$ -substituted PSII, namely, *i*) the water ligands are not coordinated to the manganese ions in the  $S_2$  state of the OEC of  $Sr^{2+}$ -substituted PSII or *ii*) the geometry of the water ligands that are coordinated at the manganese

ion(s) is strongly disordered upon replacement of the  $\text{Ca}^{2+}$  ion with  $\text{Sr}^{2+}$ . Such disorder could result in a wide distribution of the hyperfine parameters for the corresponding protons making them elusive for detection. The first possibility can be excluded based on the recent X-ray crystal structures of the OEC in the  $S_1$  state for both  $\text{Ca}^{2+}$ -containing and  $\text{Sr}^{2+}$ -substituted PSII.<sup>7, 31</sup> Moreover, the absence of the water ligands would require significant change of the electronic structure of the  $\text{Mn}_4\text{Ca}$ -oxo cluster that contradicts the EXAFS and  $^{55}\text{Mn}$  ENDOR results in literature as well as conclusions of the present study based on 2D  $^{14}\text{N}$  HYSCORE spectroscopy. Thus, we consider only the second possibility, i.e., the replacement of  $\text{Ca}^{2+}/\text{Sr}^{2+}$  significantly affects the water ligands of the  $\text{Mn}_4\text{Ca}$ -oxo cluster by an increase in the conformational freedom. The recent high-resolution X-ray crystal structure of PSII provides direct evidence that water ligands of the  $\text{Ca}^{2+}$  ion interact with the water ligands of the  $\text{Mn}_4$  ion through hydrogen bonds.<sup>7</sup> Furthermore, the structural analysis of  $\text{Sr}^{2+}$ -substituted PSII revealed that the hydrogen-bond between W2 and W3 was broken by substitution of  $\text{Ca}^{2+}$  with  $\text{Sr}^{2+}$ .<sup>29</sup> In a  $^{55}\text{Mn}$  ENDOR study by Lohmiller et al., the authors do not observe any changes in the electronic structure of the Mn ions in  $\text{Ca}^{2+}$ -depleted PSII. Despite the similarity of the Mn ions in  $\text{Ca}^{2+}$ -containing and  $\text{Ca}^{2+}$ -depleted PSII, it is known that  $\text{Ca}^{2+}$ -depleted PSII does not advance beyond  $S_2$  state in the S-state cycle. Hence, the authors suggest that the  $\text{Ca}^{2+}$  ion is likely critical for maintaining the hydrogen bond network between the redox-active tyrosine residue,  $\text{Y}_Z$ , and the  $\text{Mn}_4\text{Ca}$ -oxo cluster.<sup>57</sup> Thus, it is reasonable that the disorder of the water ligands coordinating Mn ion(s) that is observed by 2D  $^1\text{H}$  HYSCORE spectroscopy in the present study is due to disruption of the hydrogen bond network around the  $\text{Mn}_4\text{Ca}$ -oxo cluster that is caused by the increased ionic radius of the  $\text{Sr}^{2+}$  ion. Together with the differences observed by X-ray crystallography,<sup>31</sup> these structural changes might be among the main reasons for the slowing down of the catalytic turnover upon exchange

of the  $\text{Ca}^{2+}$  ion in the OEC by  $\text{Sr}^{2+}$ . It has been found that steps involving proton transfer are slower in  $\text{Sr}^{2+}$ -substituted PSII.<sup>12, 20</sup> The disruption of the hydrogen bonds between the water ligands of  $\text{Sr}^{2+}$  and Mn ion(s) observed here could potentially slow down the proton transfer. Thus, our results directly support earlier suggestions that the  $\text{Ca}^{2+}$  ion plays a structural role in maintaining hydrogen bond network that may be essential for the oxygen-evolution activity in PSII.<sup>14</sup> The ionic radius of the  $\text{Ca}^{2+}$  ion seems to play an important role for the formation of the hydrogen bond network around the multi-nuclear metal core to facilitate efficient proton transfer during the catalytic cycle. These results are in excellent agreement with the recent study by Rappaport and coworkers.<sup>14</sup> Based on the temperature dependence of the rate of the water oxidation reaction, the authors concluded that the distribution of the conformational microstates around the  $\text{Mn}_4\text{Ca}(\text{Sr})$ -oxo cluster is perturbed upon replacement of the  $\text{Ca}^{2+}$  ion by  $\text{Sr}^{2+}$  in the OEC of PSII.

## CONCLUSIONS.

In this work, we use 2D HYSCORE spectroscopy to study the weak magnetic interactions of the paramagnetic  $\text{Mn}_4\text{Sr}$ -oxo cluster and the surrounding protons in the  $S_2$  state of the OEC of  $\text{Sr}^{2+}$  substituted PSII from *T. vulcanus*. We observe a  $^{14}\text{N}$  atom that is strongly interacting with the paramagnetic  $\text{Mn}_4\text{Sr}$ -oxo cluster in the  $S_2$  state of the OEC of  $\text{Sr}^{2+}$ -substituted PSII. We assign the  $^{14}\text{N}$  atom to the imino nitrogen atom of the D1-His332 residue in the OEC of  $\text{Sr}^{2+}$ -substituted PSII. The difference in the hyperfine interaction of the directly coordinated imino nitrogen atom of histidine is negligible for  $\text{Sr}^{2+}$ -substituted and  $\text{Ca}^{2+}$ -containing PSII which indicates that the geometry of the  $\text{Mn}_4\text{Ca}(\text{Sr})$ -oxo cluster is not significantly affected by replacement of the  $\text{Ca}^{2+}$

ion by  $\text{Sr}^{2+}$ . We observe three well-resolved groups of protons,  $\text{H}^{\text{I}}$  -  $\text{H}^{\text{III}}$ , that are interacting with the  $\text{Mn}_4\text{Sr}$ -oxo cluster in the  $\text{S}_2$  state of the OEC of  $\text{Sr}^{2+}$ -substituted PSII. For each group of protons, we determine the isotropic and anisotropic component of the hyperfine tensor,  $a_{\text{iso}}$  and  $T$ , respectively that are presented in Table 1. We assign  $\text{H}^{\text{I}}$  to the two proximal protons of D1-His 332 residue. Further, we determine the spin projection factor of the Mn(III) ion of the  $\text{Mn}_4\text{Sr}$ -oxo cluster in the  $\text{S}_2$  state of the OEC as  $\rho_1 = \pm 1.7$ . This provides the first experimental determination of the spin projection factor for a Mn(III) ion. By comparing the proton hyperfine interactions of  $\text{Sr}^{2+}$ -substituted with  $\text{Ca}^{2+}$ -containing PSII, we conclude that the  $\text{Ca}^{2+}$  ion plays structural role in maintaining hydrogen bond network which may be essential for the oxygen-evolution activity of PSII.

#### ACKNOWLEDGEMENTS.

This research is supported by the Photosynthetic Systems Program, Office of Basic Energy Sciences, United States Department of Energy (DE-FG02-07ER15903) (K.V.L.) and by a Grant-in-Aid for Specially Promoted Research (No. 24000018) from MEXT/JSPS of Japan (J.R.S.).

#### REFERENCES.

1. R. J. Debus, *Biochim. Biophys. Acta*, 1992, **1102**, 269-352.
2. J. P. McEvoy and G. W. Brudvig, *Chem. Rev.*, 2006, **106**, 4455-4483.
3. J. Barber, *Q. Rev. Biophys.*, 2003, **36**, 71-89.
4. J. M. Peloquin and R. D. Britt, *Biochim. Biophys. Acta Bioenerg.*, 2001, **1503**, 96-111.
5. J. Kern and G. Renger, *Photosyn. Res.*, 2007, **94**, 183-202.

6. B. Kok, B. Forbush and M. McGloin, *Photochem. Photobiol.*, 1970, **11**, 457-475.
7. Y. Umena, K. Kawakami, J. R. Shen and N. Kamiya, *Nature*, 2011, **473**, 55-60.
8. A. Boussac, J. L. Zimmermann and A. W. Rutherford, *Biochemistry*, 1989, **28**, 8984-8989.
9. M. Sivaraja, J. Tso and G. C. Dismukes, *Biochemistry*, 1989, **28**, 9459-9464.
10. C. F. Yocum, *Biochim. Biophys. Acta*, 1991, **1059**, 1-15.
11. G. M. Ananyev, L. Zaltsman, C. Vasko and G. C. Dismukes, *Biochim. Biophys. Acta Bioenerg.*, 2001, **1503**, 52-68.
12. A. Boussac and A. W. Rutherford, *Biochemistry*, 1988, **27**, 3476-3483.
13. D. F. Ghanotakis, G. T. Babcock and C. F. Yocum, *FEBS Lett.*, 1984, **167**, 127-130.
14. F. Rappaport, N. Ishida, M. Sugiura and A. Boussac, *Energ. Environ. Sci.*, 2011, **4**, 2520-2524.
15. G. Hendry and T. Wydrzynski, *Biochemistry*, 2003, **42**, 6209-6217.
16. J. S. Vrettos, D. A. Stone and G. W. Brudvig, *Biochemistry*, 2001, **40**, 7937-7945.
17. J. P. McEvoy and G. W. Brudvig, *Phys. Chem. Chem. Phys.*, 2004, **6**, 4754-4763.
18. E. M. Sproviero, K. Shinopoulos, J. A. Gascon, J. P. McEvoy, G. W. Brudvig and V. S. Batista, *Philos. Trans. R. Soc. London, Ser. B*, 2008, **363**, 1149-1156.
19. A. Boussac, F. Rappaport, P. Carrier, J. M. Verbavatz, R. Gobin, D. Kirilovsky, A. W. Rutherford and M. Sugiura, *J. Biol. Chem.*, 2004, **279**, 22809-22819.
20. Y. L. Pushkar, J. Yano, K. Sauer, A. Boussac and V. K. Yachandra, *Proc. Natl. Acad. Sci. U. S. A.*, 2008, **105**, 1879-1884.
21. M. A. Strickler, L. M. Walker, W. Hillier and R. J. Debus, *Biochemistry*, 2005, **44**, 8571-8577.

22. H. Suzuki, Y. Taguchi, M. Sugiura, A. Boussac and T. Noguchi, *Biochemistry*, 2006, **45**, 13454-13464.
23. Y. Kimura, K. Hasegawa and T. Ono, *Biochemistry*, 2002, **41**, 5844-5853.
24. N. Cox, L. Rapatskiy, J.-H. Su, D. A. Pantazis, M. Sugiura, L. Kulik, P. Dorlet, A. W. Rutherford, F. Neese, A. Boussac, W. Lubitz and J. Messinger, *J. Am. Chem. Soc.*, 2011, **133**, 3635-3648.
25. V. K. Yachandra and J. Yano, *J. Photochem. Photobiol. B*, 2011, **104**, 51-59.
26. T. Ono, A. Rompel, H. Mino and N. Chiba, *Biophys. J.*, 2001, **81**, 1831-1840.
27. C. F. Yocum, *Coord. Chem. Rev.*, 2008, **252**, 296-305.
28. G. Hendry and T. Wydrzynski, *Biochemistry*, 2002, **41**, 13328-13334.
29. W. Hillier and T. Wydrzynski, *Biochemistry*, 2000, **39**, 4399-4405.
30. K. L. Westphal, N. Lydakis-Simantiris, R. I. Cukier and G. T. Babcock, *Biochemistry*, 2000, **39**, 16220-16229.
31. F. H. M. Koua, Y. Umena, K. Kawakami and J.-R. Shen, *Proc. Natl. Acad. Sci. U. S. A.*, 2013, **110**, 3889-3894.
32. S. Milikisiyants, R. Chatterjee, A. Weyers, A. Meenaghan, C. Coates and K. V. Lakshmi, *J. Phys. Chem. B*, 2010, **114**, 10905-10911.
33. S. Milikisiyants, R. Chatterjee, C. S. Coates, F. H. M. Koua, J.-R. Shen and K. V. Lakshmi, *Energ. Environ. Sci.*, 2012, **5**, 7747-7756.
34. J. R. Shen and Y. Inoue, *Biochemistry*, 1993, **32**, 1825-1832.
35. J. R. Shen, M. Ikeuchi and Y. Inoue, *FEBS Lett.*, 1992, **301**.
36. W. F. Beck, J. C. Depaula and G. W. Brudvig, *Biochemistry*, 1985, **24**, 3035-3043.
37. G.W. Brudvig, *Adv. Chem. Series*, 1995, **246**, 249-263.

38. G. W. Brudvig, *ACS Symp. Ser.*, 1988, **372**, 221-237.
39. J. C. Depaula, W. F. Beck and G. W. Brudvig, *J. Am. Chem. Soc.*, 1986, **108**, 4002-4009.
40. M. Zheng and G. C. Dismukes, *Inorg. Chem.*, 1996, **35**, 3307-3319.
41. R. Chatterjee, S. Milikisiyants and K. V. Lakshmi, *Phys. Chem. Chem. Phys.*, 2012, **14**.
42. S. Milikisiyants, R. Chatterjee and K. V. Lakshmi, *J. Phys. Chem. B*, 2011, **115**, 12220-12229.
43. R. Chatterjee, S. Milikisiyants, C. S. Coates and K. V. Lakshmi, *Biochemistry*, 2011, **50**, 491-501.
44. N. Srinivasan, R. Chatterjee, S. Milikisiyants, J. H. Golbeck and K. V. Lakshmi, *Biochemistry*, 2011, **50**, 3495-3501.
45. G.W. Brudvig, *Adv. Chem. Series*, 1995, **246**, 249-263.
46. N. Cox, L. Rapatskiy, J.-H. Su, D. A. Pantazis, M. Sugiura, L. Kulik, P. Dorlet, A. W. Rutherford, F. Neese, A. Boussac, W. Lubitz and J. Messinger, *J. Am. Chem. Soc.*, 2011, **133**, 14149-14149.
47. S. A. Dikanov, L. Y. Xun, A. B. Karpel, A. M. Tyryshkin and M. K. Bowman, *J. Am. Chem. Soc.*, 1996, **118**, 8408-8416.
48. G. J. Yeagle, M. L. Gilchrist, R. M. McCarrick and R. D. Britt, *Inorg. Chem.*, 2008, **47**, 1803-1814.
49. C. Teutloff, S. Pudollek, S. Kessen, M. Broser, A. Zouni and R. Bittl, *Phys. Chem. Chem. Phys.*, 2009, **11**, 6715-6726.
50. R. J. Debus, K. A. Campbell, W. Gregor, Z. L. Li, R. L. Burnap and R. D. Britt, *Biochemistry*, 2001, **40**, 3690-3699.

51. T. A. Stich, G. J. Yeagle, R. J. Service, R. J. Debus and R. D. Britt, *Biochemistry*, 2011, **50**, 7390-7404.
52. M. P. Navarro, W. M. Ames, H. Nilsson, T. Lohmiller, D. A. Pantazis, L. Rapatskiy, M. M. Nowaczyk, F. Neese, A. Boussac, J. Messinger, W. Lubitz and N. Cox, *Proc. Natl. Acad. Sci. U. S. A.*, 2013, **110**, 15561-15566.
53. P. E. M. Siegbahn, *Acc. Chem. Res.*, 2009, **42**, 1871-1880.
54. J. M. Peloquin, K. A. Campbell, D. W. Randall, M. A. Evanchik, V. L. Pecoraro, W. H. Armstrong and R. D. Britt, *J. Am. Chem. Soc.*, 2000, **122**, 10926-10942.
55. S. Schinzel, J. Schraut, A. V. Arbuznikov, P. E. M. Siegbahn and M. Kaupp, *Chemistry Eur. J.*, 2010, **16**, 10424-10438.
56. L. V. Kulik, B. Epel, W. Lubitz and J. Messinger, *J. Am. Chem. Soc.*, 2007, **129**, 13421-13435.
57. T. Lohmiller, N. Cox, J. H. Su, J. Messinger and W. Lubitz, *J. Biol. Chem.*, 2012, **287**, 24721-24733.

**TABLES.**

**Table 1.** The  $^1\text{H}$  hyperfine interaction parameters obtained by spectral simulations of the 2D  $^1\text{H}$  HYSCORE spectrum of the  $S_2$  state of the OEC of  $\text{Sr}^{2+}$ -substituted PSII (Figure 3). The error bars are indicated in parentheses.

**Table 1**

<b>Ridge</b>	<b>T , MHz</b>	<b>a<sub>iso</sub> , MHz</b>
<b>H<sup>I</sup></b>	$\pm 4.1 (\pm 0.2)$	$\sim 0 (\pm 0.2)$
<b>H<sup>II</sup></b>	$\pm 2.2 (\pm 0.2)$	$\pm 0.2 (\pm 0.2)$
<b>H<sup>III</sup></b>	$\pm 1.5 (\pm 0.4)$	$\pm 0.2 (\pm 0.4)$

**FIGURE CAPTIONS.**

**Figure 1.** The pulsed electron spin-echo-detected magnetic-field-sweep EPR spectrum of the  $S_2$  state of the OEC of  $\text{Sr}^{2+}$ -substituted PSII from *T. vulcanus*.

\*The region of the spectrum containing the EPR signal from the  $\text{Y}_D^\bullet$  radical.

\*\* The region of the spectrum containing unavoidable resonator artifacts.

**Figure 2.** The 2D  $^{14}\text{N}$  HYSCORE spectrum of the  $S_2$  state of the OEC of (A)  $\text{Sr}^{2+}$ -substituted PSII and (B)  $\text{Ca}^{2+}$ -containing PSII from *T. vulcanus*. The spectrum was acquired at a magnetic field position corresponding to a  $g$  value of 1.95 with a  $\tau$  delay of 140 ns.

**Figure 3.** The 2D  $^1\text{H}$  HYSCORE spectrum of the  $S_2$  state of the OEC of  $\text{Sr}^{2+}$ -substituted PSII from *T. vulcanus*. The spectrum was acquired at a magnetic field position corresponding to a  $g$  value of 1.95 with a  $\tau$  delay of 140 ns.

**Figure 4.** The 2D  $^1\text{H}$  HYSCORE spectrum of the  $S_2$  state of the OEC of  $\text{Ca}^{2+}$ -containing PSII from *T. vulcanus*. The spectrum was acquired at a magnetic field position corresponding to a  $g$  value of 1.95 with a  $\tau$  delay of 140 ns.<sup>33</sup>

**Figure 5.** The structure of the  $\text{Mn}_4\text{Ca}$ -oxo cluster, as seen in the X-ray crystal structure of PSII.<sup>24</sup> Shown are the protons of the four water molecules that are coordinated at the manganese and calcium ions of the cluster, the nine water molecules in the hydrogen-bond network and the D1-His332, D1-His337 and CP43-Arg357 residues, respectively, that are in the vicinity of the  $\text{Mn}_4\text{Ca}$ -oxo cluster.

## FIGURES.

Figure 1.

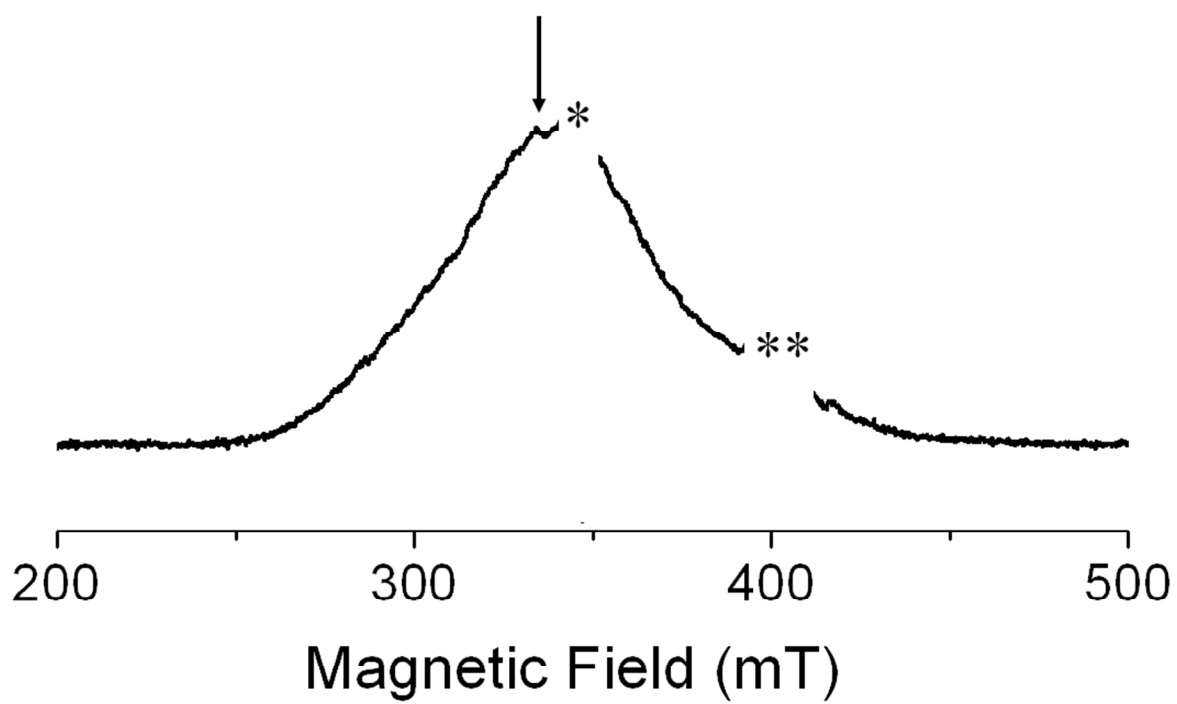


Figure 2.

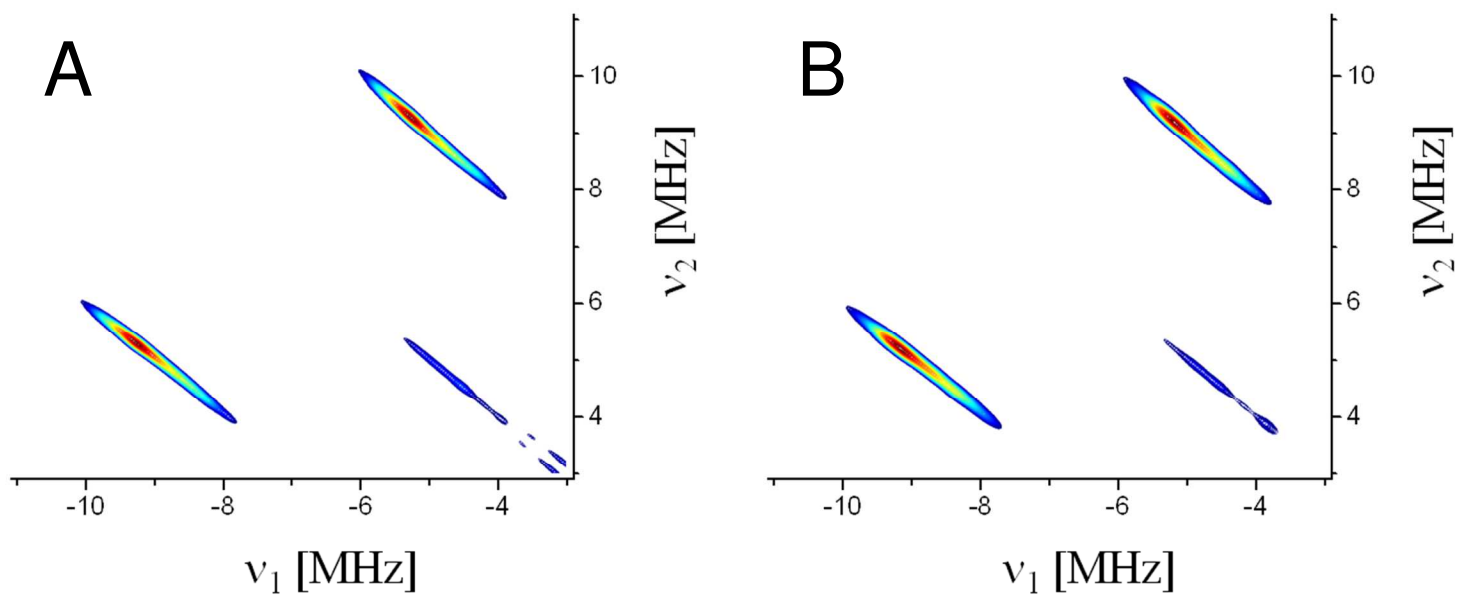


Figure 3.

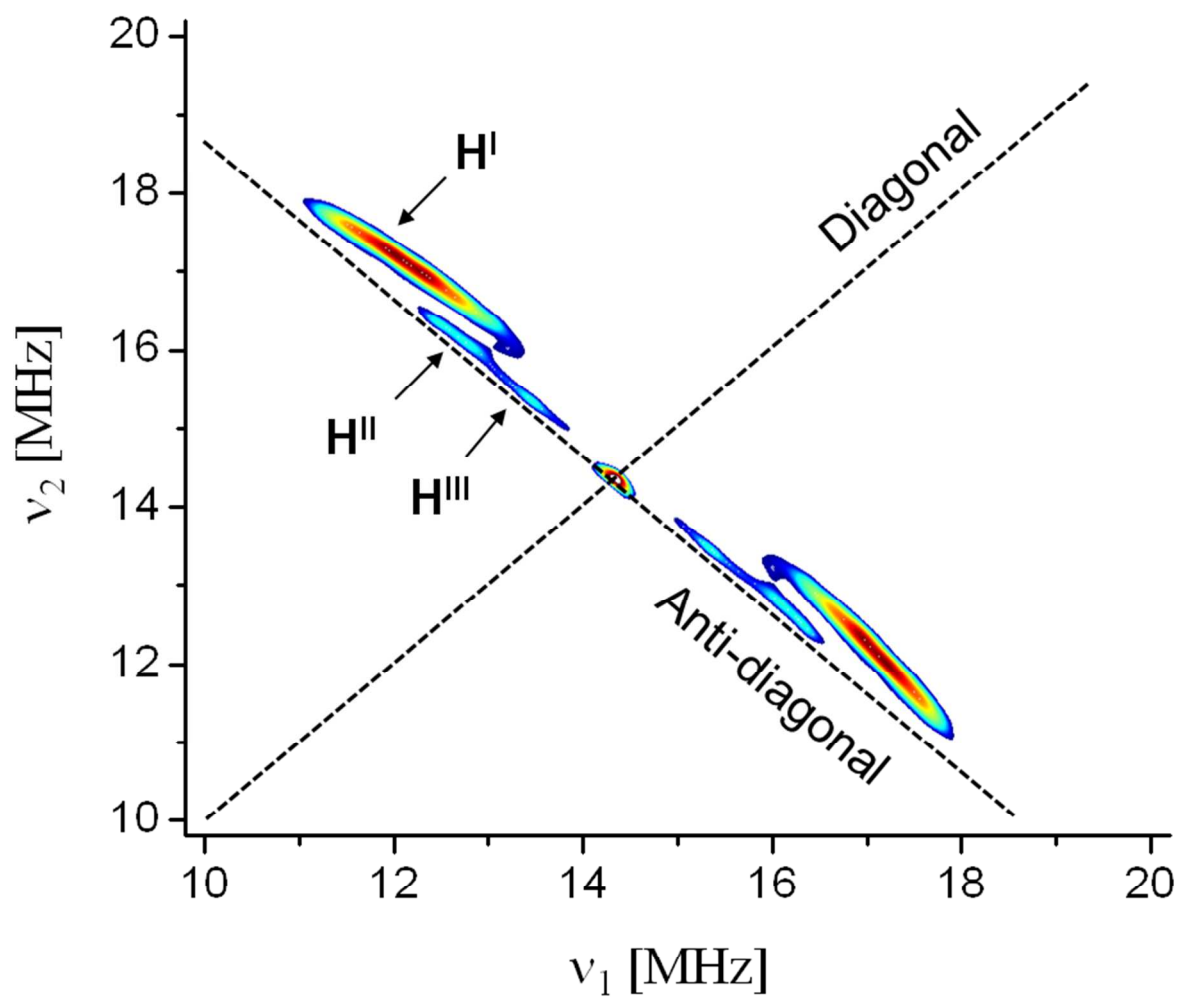


Figure 4.

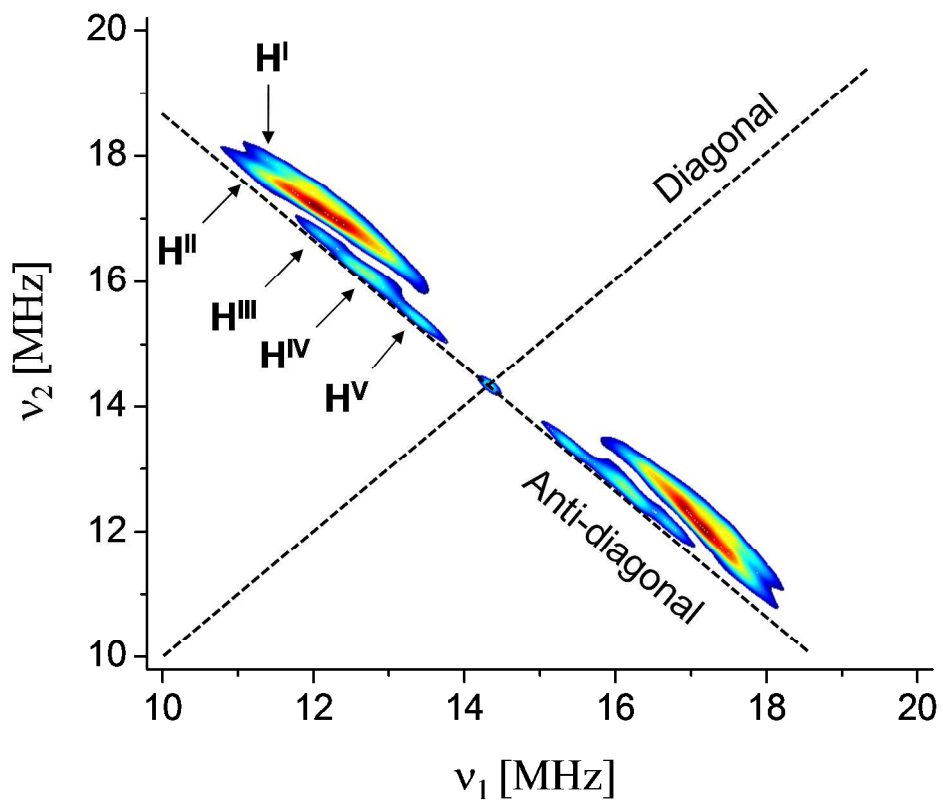


Figure 5.

